Virologica Sinica 37 (2022) 469–471

Contents lists available at ScienceDirect

Virologica Sinica

journal homepage: www.keaipublishing.com/en/journals/virologica-sinica
www.virosin.org

Letter

Construction and verification of an infectious cDNA clone of coxsackievirus B5

Lifang Song [a,1], Bopei Cui [a,b,1], Jinghuan Yang [a], Xiaotian Hao [a], Xujia Yan [a], Jialu Zhang [a], Dong Liu [a], Ziyang Song [a], Qian Wang [a], Qunying Mao [a,*], Zhenglun Liang [a,*]

[a] National Institute for Food and Drug Control, Beijing 102629, China
[b] Wuhan Institute of Biological Products CO., LTD, Wuhan 430070, China

Dear Editor,

Enteroviruses belonging to the family *Picornaviridae* are non-enveloped RNA viruses that cause hand-foot-mouth disease (HFMD), which can lead to severe neurological complications. Enteroviruses genomes represent a single open reading frame flanked by 5′-and 3′-untranslated terminal regions (UTRs), constituting the basis for classifying enteroviruses into groups A–D (Zaoutis et al., 1998). Current research is primarily focused on highly prevalent pathogens, including enterovirus A71 (EV-A71) and coxsackievirus A16 (CV-A16) of group A (Duan et al., 2021). However, group B viruses are also responsible for a significant number of infections that often cause histopathological changes in the heart, brain, and pancreas. For instance, coxsackievirus B5 (CV-B5) can induce aseptic meningitis, viral meningitis, acute flaccid paralysis, pancreatitis, and type I diabetes mellitus (Chen et al., 2020; Françozo et al., 2019; Hyöty et al., 2018). HFMD outbreaks caused by CV-B5 have been reported in China, Southeast Asia, and Europe. However, despite its clinical significance, little is known about its pathogenesis, and in-depth studies on the underlying mechanisms are urgently needed (Gao et al., 2018; Sciandra et al., 2020).

Reverse genetics is a conventional method for studying the pathogenesis and virulence of viruses (Hao et al., 2021; Ding et al., 2021). Recently, complementary DNA (cDNA) clones of CV-B3, CV-A10, CV-A6, CV-A16, EV-A71, and EV-D68 have been constructed, and the biological characteristics of the rescued viruses have been validated (Liu et al., 2019; Ma et al., 2015; Yang et al., 2015; Pan et al., 2018; Wang et al., 2020). However, cDNA clones of CV-B5 have not yet been reported. Here, we describe the construction of a CV-B5 cDNA clone and characterization of the rescued live virus, which shows virulence comparable to that of the parental virus and causes similar symptoms in mice.

To construct a full-length infectious cDNA clone of CV-B5 (GenBank No. AF114383), the whole genome was amplified in two segments (primers shown in Supplementary Table S1). Segment I (3300 nt) consisted of a 36 nt fragment (8 nt + *Not*I cleavage site + T7 RNA polymerase promoter) upstream of the pSVA vector 5′-UTR, the viral genome 5′-UTR, and the sequence coding for CV-B5 structural protein 1 (P1), whereas segment II (4200 nt) consisted of a 20 nt pSVA fragment (14 nt + *Sal*I site), a 3278–7400 nt fragment comprising CV-B5 non-structural protein 2 (P2), the non-structural protein 3 (P3), the 3′-UTR sequences, and a 38 bp poly A tail (Fig. 1A, Supplementary Fig. S1A). The two segments were seamlessly inserted into the pSVA vector using the In-Fusion Cloning Kit (Cat#639649, Clontech, USA), and the resulting pSVA-CV-B5-cDNA plasmid was verified by restriction endonuclease digestion (Supplementary Fig. S1B) and sequencing.

Infectious clones are often used for virus rescue, and the acquired viruses can be verified based on their biological characteristics such as cytopathic effect (CPE), virus titer, and growth kinetics. Thus, a rescued tick-borne encephalitis virus induces phagocytosis in BHK-21 cells and shows the CPE and growth curves similar to those of parental viruses (Li et al., 2021). In this study, we rescued the virus by inoculating pSVA-CV-B5-cDNA and a T7 RNA polymerase-expressing plasmid into HEK 293T cells, and then propagating the virus in Vero cells. The virus-containing supernatant was designated as the first-generation rescued virus (G1) and its titer was similar to that of the parental strain (3.16×10^8 $TCID_{50}$/mL vs. 5.12×10^8 $TCID_{50}$/mL).

To compare growth kinetics of the rescued and parental viruses, they were used to infect Vero cells at a multiplicity of infection (MOI) of 0.01, and viral titers in the supernatant were monitored every 12 h for 5 days. There was an almost identical time-dependent increase in the titers of both viruses, which at 60 hpi reached a plateau (1×10^8 $TCID_{50}$/mL) persisting until the end of the experiment, indicating that the infection progression was similar for the rescued and parental viruses (Fig. 1B). In rescued virus-infected Vero cells, a typical CPE was first noted at 24 h post-infection (hpi), which became noticeable at 48 hpi, when a large number of shrinking, aggregating, and floating cells were observed, indicating that the CPE of the rescued virus was similar to that of the parental virus (Fig. 1C–E).

* Corresponding authors.
E-mail addresses: maoqunying@126.com (Q. Mao), lzhenglun@126.com (Z. Liang).
[1] Lifang Song and Bopei Cui contributed equally to this work.

https://doi.org/10.1016/j.virs.2022.03.005
Received 7 September 2021; Accepted 7 March 2022
Available online 11 March 2022

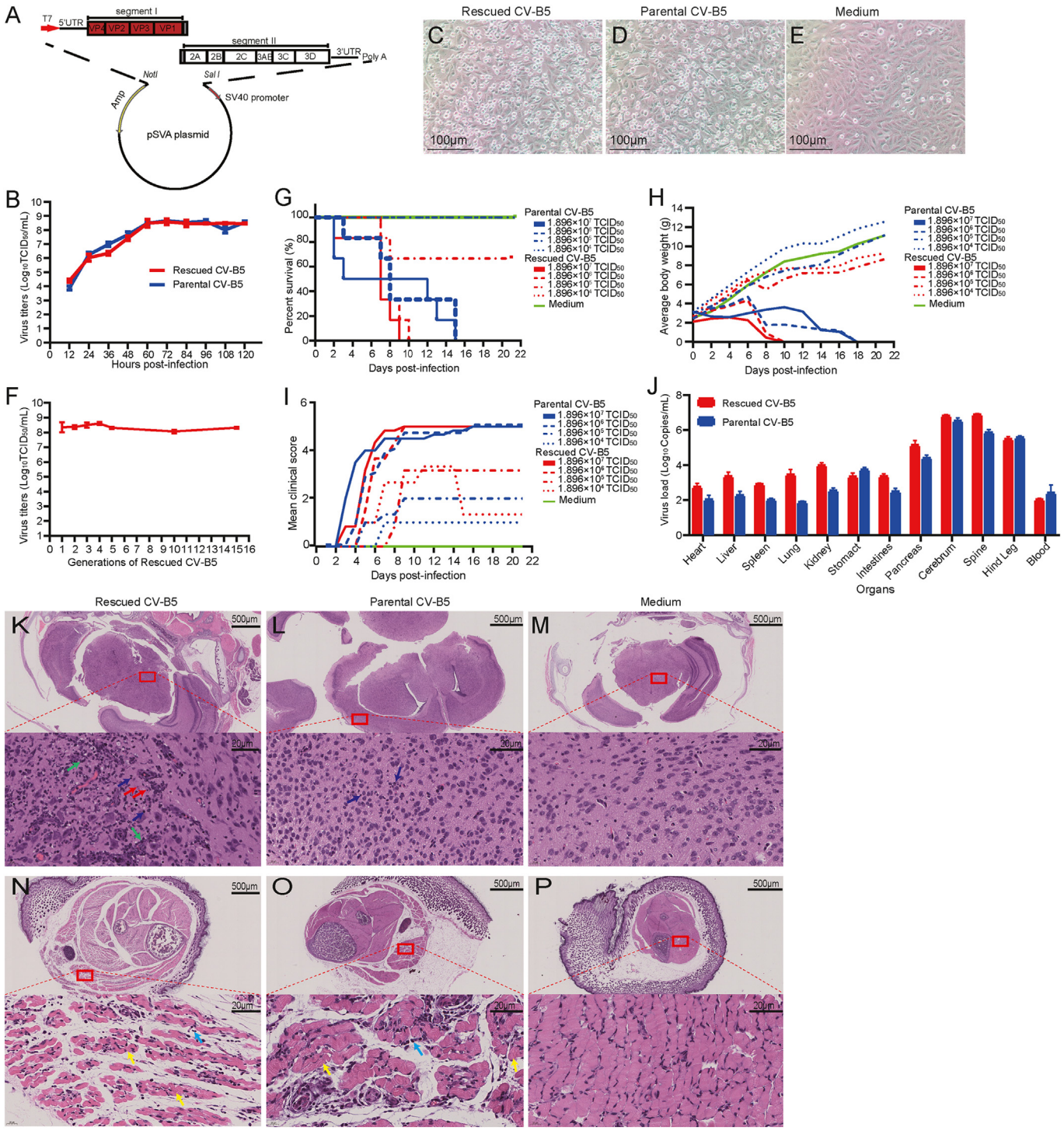

Fig. 1. Construction and verification of the full-length cDNA clone of CV-B5 and the rescued virus. **A** The construction scheme of the full-length CV-B5 cDNA clone. Segment I (3300 nt) consisted of *Not*I cleavage site, T7 RNA polymerase promoter, the 5′-UTR of viral genome, and the sequence coding for CV-B5 structural protein 1 (P1), whereas segment II (4200 nt) consisted of *Sal*I site, non-structural protein 2 (P2), non-structural protein 3 (P3), and the 3′-UTR sequences. **B** Characteristics of the growth kinetics of CV-B5 rescued and parental viruses cultured in Vero cells for 5 days. The viral titer was detected at a 12 h interval shown as $TCID_{50}$. **C–E** Verification of CV-B5 rescued virus in Vero cell, CPE of Vero cell induced by the rescued virus (**C**), parental virus (**D**) and medium (**E**), respectively. **F** CV-B5 rescued virus was serially passaged on Vero cells, and passage 1–5, 10, and 15 were selected for viral titer detection. **G–I** Survival rate (**G**), average body weight (**H**) and mean clinical score (**I**) of suckling mice after challenge by CV-B5 rescued or parental viruses (n = 6). The LD_{50} of parental and rescued CV-B5 were 9.71×10^5 and 3.37×10^5 $TCID_{50}$, respectively. Clinical scoring was as follows: 0 health; 1 wasting; 2 forelimb paralysis; 3 paralysis of the hind limbs; 4 quadriplegia; and 5 moribund status or death. **J** Distribution of CV-B5 rescued and parent virus in various tissues and organs (n = 3). Real-time PCR was used to detect the viral load in 12 organs or tissues including heart, liver, spleen, lung, kidney, stomach, intestine, pancreas, cerebrum, spine, hind leg, and blood. The results of the control group were under the detection limit. **K–P** Histopathological changes of the cerebrum (**K–M**) and hind leg (**N–P**) caused by CV-B5 rescued and parental virus. Inflammatory cell infiltration, mostly neutrophils, was seen around the cerebral cortex nerve cells (blue arrows); glial cells showed hyperplasia in the brain (green arrows); and skeletal muscles and muscle fibers manifested swelling, degeneration, necrosis (yellow arrows), and infiltration by inflammatory cells in matrix (sky blue arrows).

Next, we investigated the stability of the rescued virus genome over generations and its reproduction ability. The G1 rescued virus was serially passaged in Vero cells, and the whole genomes of G1, G5, G10, and G15 viruses were sequenced. No mutations occurred across the generations, suggesting that the rescued CV-B5 virus was genetically stable. Measurements of the G1–G5, G10, and G15 viral titers showed that all generations could reach 1×10^8 $TCID_{50}$/mL, suggesting a robust ability of the recombinant virus to replicate and assemble progeny (Fig. 1F). Comparison of CPEs, infectious doses, and growth kinetics between the rescued and parental viruses indicated that the two strains possessed similar biological characteristics.

In addition to exhibiting parent virus-like characteristics in *in vitro* infection, the rescued virus should also be verified for pathogenicity in susceptible *in vivo* models. Studies of group A rescued coxsackieviruses in a neonatal mouse model indicate that rescued CV-A6 causes typical symptoms of reduced mobility, wasting, limb weakness, and paralysis at 3 days post-infection (dpi), whereas rescued CV-A10 can cause scattering of limb skeletal muscle fibers, intestinal villus interstitial edema, and alveolar shrinkage (Yang et al., 2015; Liu et al., 2019). Group B coxsackieviruses cause neurological symptoms in mice more often than group A. Three-day-old BALB/c mice infected intraperitoneally (i.p.) with 26 LD_{50} (3.16×10^3 $TCID_{50}$) of CV-B5/JS417 (GenBank No. KY303900.1) show necrosis of neuronal cells in the cerebral cortex and spinal cord, and necrotizing myositis in hind legs (Mao et al., 2018). The parental and rescued viruses were serially diluted 10-fold (starting from 1.896×10^7 $TCID_{50}$) to i.p. infect 3-day-old BALB/c suckling mice, whose survival rate (Fig. 1G), body weight (Fig. 1H), and clinical symptoms (Fig. 1I) were recorded for 21 days. The LD_{50} of the rescued and parental viruses were 3.37×10^5 and 9.71×10^5 $TCID_{50}$, respectively. The 1.896×10^7 and 1.896×10^6 $TCID_{50}$ dosages of the rescued and parental viruses, respectively, caused a dramatic decrease in the average weight (Fig. 1H) and led to death in all mice of the respective groups (Fig. 1G). The two lower dosages caused a marginal reduction in mouse weight compared to the control (Fig. 1H). In mice challenged with the same dosage (Fig. 1G), the survival rate of the rescued and parental viruses showed no difference ($P > 0.05$). We further analyzed the symptoms of the infected mice and calculated clinical scores. The mice showed clinical symptoms within 3–4 days after challenge with the two higher dosages of the rescued or parental viruses, respectively (Fig. 1I). Apparent clinical symptoms such as weight loss, lack of energy, tremor, rickets, and hind limb paralysis were observed at 5 dpi. The highest average clinical score (5 points) was recorded on days 9 and 10 for the rescued virus-infected group and on days 14 and 15 for the parental virus-infected group. Those results indicated that the virulence of the rescued virus was not weaker than that of the parental virus.

To investigate tissue tropism of the viruses, we infected 3-day-old BALB/c mice with the same dose (1.896×10^7 $TCID_{50}$) of the rescued and parental viruses, respectively, and analyzed the viral load after 5 days. The viruses were detected in 12 different organs and tissues, including the heart, liver, spleen, lung, kidney, stomach, intestine, pancreas, cerebrum, spine, hind legs, and blood. Tissue and organ distribution of rescued viruses were consistent with that of parental viruses; the highest viral load was detected in the spine, cerebrum, hind legs, and pancreas, followed by the stomach, kidney, intestine, heart, and liver (Fig. 1J). Viral loads in cerebrum, pancreas, hind leg, blood, stomach and heart of the two groups showed no difference ($P > 0.05$). While viral loads manifested differences in spine ($P = 0039$), lung ($P < 0.0001$), kidney ($P < 0.0001$), liver ($P = 0.0013$), spleen ($P = 0.0146$), and intestine ($P = 0.0183$), the distribution and tissue tropism were in agreement.

Histopathological analysis revealed glial cells hyperplasia (green arrows), inflammatory cell infiltration (blue arrows), and scattered nerve cell necrosis (red arrows) in the brain of the rescued virus group (Fig. 1K), and that inflammatory cell infiltration (mostly neutrophils) was observed around the cerebral cortex nerve cells in the parental virus group (Fig. 1L), with no histopathological changes seen in the control (injected with medium) group (Fig. 1M). Skeletal muscles and muscle fibers of hind legs in the rescued virus (Fig. 1N) and parental virus (Fig. 1O) groups showed swelling, degeneration, necrosis (yellow arrows), and inflammatory cell infiltration into the matrix (sky blue arrows), whereas no such changes were observed in the control group (Fig. 1P). Both rescued and parental CV-B5 could breach the blood-brain barrier and enter the brain tissue to replicate, causing nerve damage and inflammation, and that the two strains induce similar pathological changes in the brain and hind leg muscles.

In conclusion, we report the construction of the first stable cDNA clone of CV-B5, encoding an infectious recombinant virus, which is biologically and functionally similar to the parental strain. Our results provide a framework for future studies on the determinants of virulence and pathogenicity of coxsackieviruses and could be useful for the development of attenuated virus vaccines and therapeutic drugs.

Footnotes

This work was supported by the National Key Research and Development Project (grant number 2018ZX09737-011). The authors declare that they have no conflict of interest. Animal Research was conducted in compliance with the Animal Welfare Act, approval was granted by the Ethics Committee of the National Institute for Food and Drug Control (NO. 2020(B) 018). All institutional and national guidelines for the care and use of laboratory animals were followed.

Supplementary data to this article can be found online at https://doi.org/10.1016/j.virs.2022.03.005.

References

Chen, Y., Yang, S., Yang, H., Lin, T., Hsieh, Y., Arthur Huang, K., Kuo, C., Chiu, C., Huang, Y., Chu, S., Chen, J., 2020. Clinical characteristics of echovirus 11 and coxsackievirus B5 infections in Taiwanese children requiring hospitalization. J. Microbiol. Immunol. Infect. S1684–1182, 30149–30153.

Ding, L., Brown, D., Glass, J., 2021. Rescue of infectious sindbis virus by yeast spheroplast-mammalian cell fusion. Viruses 13, 603.

Duan, X., Chen, Z., Li, X., Ping, Y., Lu, L., 2021. Virus shedding in patients with hand, foot and mouth disease induced by EV71, CA16 or CA6: systematic review and meta-analysis. Pediatr. Infect. Dis. J. 40, 289–294.

Françozo, M., Costa, F., Guerra-Gomes, I., Silva, J., Sesti-Costa, R., 2019. Dendritic cells and regulatory T cells expressing CCR4 provide resistance to coxsackievirus B5-induced pancreatitis. Sci. Rep. 9, 14766.

Gao, F., Bian, L., Hao, X., Hu, Y., Yao, X., Sun, S., Chen, P., Yang, C., Du, R., Li, J., Zhu, F., Mao, Q., Liang, Z., 2018. Seroepidemiology of coxsackievirus B5 in infants and children in Jiangsu province, China. Hum Vaccin Immunother 14, 74–80.

Hyöty, H., Leon, F., Knip, M., 2018. Developing a vaccine for type 1 diabetes by targeting coxsackievirus B. Expert Rev. Vaccines 17, 1071–1083.

Hao, X., Song, S., Zhong, Q., Jamal-U-Ddin, H., Guo, J., Wu, Y., 2021. Rescue of an infection clone of barley yellow dwarf virus –GAV. Phytopathology 111, 2383–2391.

Li, P., Yao, C., Wang, T., Wu, T., Yi, W., Zheng, Y., Miao, Y., Sun, J., Tan, Z., Liu, Y., Zhang, X., Wang, H., Zheng, Z., 2021. Recovery of a far-eastern strain of tick-borne encephalitis virus with a full-length infectious cDNA clone. Virol. Sin. 36, 1375–1386.

Liu, Q., Dan, H., Zhao, X., Chen, H., Chen, Y., Zhang, N., Mo, Z., Liu, H., 2019. Construction and characterization of an infectious cDNA clone of coxsackievirus A 10. Virol. J. 16, 98.

Ma, Y., Hao, S., Sun, L., Li, J., Qiao, Q., Gao, F., Zhao, L., Yu, X., Wang, Z., Wen, H., 2015. Construction and characterization of infectious cDNA clones of enterovirus 71 (EV71). Virol. Sin. 30, 305–308.

Mao, Q., Hao, X., Hu, Y., Du, R., Lang, S., Bian, L., Gao, F., Yang, C., Cui, B., Zhu, F., Shen, L., Liang, Z., 2018. A neonatal mouse model of central nervous system infections caused by Coxsackievirus B5. Emerg. Microb. Infect. 7, 185.

Pan, M., Gao, S., Zhou, Z., Zhang, K., Liu, S., Wang, Z., Wang, T., 2018. A reverse genetics system for enterovirus D68 using human RNA polymerase I. Virus Gene. 54, 484–492.

Sciandra, I., Falasca, F., Maida, P., 2020. Seroprevalence of group B coxsackieviruses: retrospective study in an Italian population. J. Med. Virol. 92, 3138–3143.

Wang, M., Yan, J., Zhu, L., Wang, M., Liu, L., Yu, R., Chen, M., Xun, J., Zhang, Y., Yi, Z., Zhang, S., 2020. The establishment of infectious clone and single round infectious particles for coxsackievirus A10. Virol. Sin. 35, 426–435.

Yang, L., Li, S., Liu, Y., Hou, W., Lin, Q., Zhao, H., Xu, L., He, D., Ye, X., Zhu, H., Cheng, T., Xia, N., 2015. Construction and characterization of an infectious clone of coxsackievirus A6 that showed high virulence in neonatal mice. Virus Res. 210, 165–168.

Zaoutis, T., Klein, J., 1998. Enterovirus infections. Pediatr. Rev. 19, 183–191.